LBL-12411
Preprint c.2

Lawrence Berkeley Laboratory
UNIVERSITY OF CALIFORNIA

Materials & Molecular Research Division

RECEIVED
BERKELEY LABORATORY
JUL 17
LIBRARY AND DOCUMENTS SECTION

Submitted to Surface Science

THE STRUCTURE AND STABILITY OF SURFACE PLATINUM OXIDE AND OF OXIDES OF OTHER NOBLE METALS

M. Salmerón, L. Brewer, and G.A. Somorjai

April 1981

TWO-WEEK LOAN COPY
This is a Library Circulating Copy which may be borrowed for two weeks. For a personal retention copy, call Tech. Info. Division, Ext. 6782.

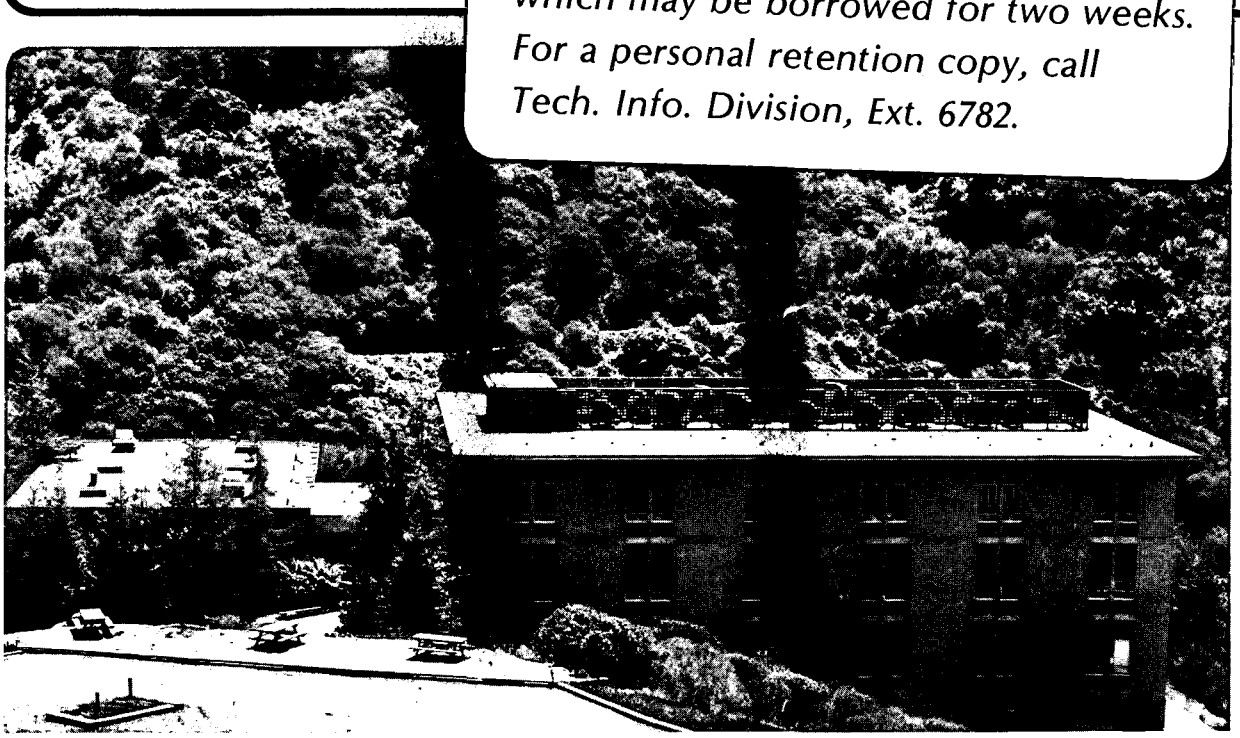

Prepared for the U.S. Department of Energy under Contract W-7405-ENG-48

LBL-12411 c.2

DISCLAIMER

This document was prepared as an account of work sponsored by the United States Government. While this document is believed to contain correct information, neither the United States Government nor any agency thereof, nor the Regents of the University of California, nor any of their employees, makes any warranty, express or implied, or assumes any legal responsibility for the accuracy, completeness, or usefulness of any information, apparatus, product, or process disclosed, or represents that its use would not infringe privately owned rights. Reference herein to any specific commercial product, process, or service by its trade name, trademark, manufacturer, or otherwise, does not necessarily constitute or imply its endorsement, recommendation, or favoring by the United States Government or any agency thereof, or the Regents of the University of California. The views and opinions of authors expressed herein do not necessarily state or reflect those of the United States Government or any agency thereof or the Regents of the University of California.

LBL 12411

THE STRUCTURE AND STABILITY OF SURFACE PLATINUM OXIDE AND OF OXIDES OF OTHER NOBLE METALS

M. Salmerón,* L. Brewer, and G.A. Somorjai

Materials and Molecular Research Division, Lawrence Berkeley Laboratory
and
Department of Chemistry, University of California, Berkeley, CA 94720

Abstract

The formation and stability of surface layers of platinum oxides in platinum single crystals has been studied in ultrahigh vacuum. Low energy electron diffraction (LEED) was used to identify the ordered structures that formed on the surface of Pt(111), Pt(332), and Pt(110). It appears that these structures can be related to hexagonal planes of PtO_2. The cleanliness of the surface was monitored by Auger electron spectroscopy (AES). The presence of impurities like Ca and Si must be avoided as they oxidize preferentially to the Pt. It is shown that the Pt oxide layers are stabilized by the very slow kinetics of oxygen diffusion to the surface which is responsible for the observed long life of the oxide layers under most catalytic reactions that are carried out at temperatures below 500°C. The stability of other oxides of noble metals that have been observed in UHV studies is also reviewed.

*Permanent address: Instituto de Física del Estado Sólido del CSIC
Universidad Autónoma de Madrid, Spain

This work was supported by the Director, Office of Energy Research, Office of Basic Energy Sciences, Materials Sciences Division of the U.S. Department of Energy under Contract W-7405-ENG-48.

Introduction

The formation of platinum oxide and oxides of other noble metals has often been studied in the presence of gas phase oxygen (1-3) and at metal surfaces in aqueous solution (4-6). The oxidized surfaces exhibit unique chemical properties that are frequently utilized in heterogeneous catalysis (7-9) and for electrode reactions (4). There are many reports of platinum oxide formation in the near surface region of metal single crystals in high vacuum surface studies (10-13). These surface oxides can be produced by heating platinum at high temperatures, 800-1000°C, in a low partial pressure of oxygen, 10^{-7}-10^{-5} Torr and then cooling the sample to 25°C in vacuum or in the low pressure of oxygen. It should be noted here, and it will be discussed later in this paper, that the oxygen pressures employed to produce the oxide are much lower than the dissociation pressure of platinum oxide that can be calculated from the available thermodynamic data. Thus the oxide should not be stable and should not form, based on these thermodynamic considerations. In fact, two recent papers (14,15) blame all observation of noble metal oxides reported to exist in the near surface regions to be due to oxides of impurities that were dissolved in noble metals (calcium and silicon, principally). Oxides of other noble metals, (iridium (16,17), rhodium, (18), palladium (19), and gold (20)) have also been produced and studied. For these metals the bulk oxides exhibit low thermodynamic stability just as the platinum oxides. However, once formed, the surface oxide layers appear to be stable under most conditions of the chemical studies they are subjected to, that usually do not exceed 400°C for catalytic studies and in atmospheric pressures of reducing gases of H_2, CO, and hydrocarbons.

In this paper we report the structures of platinum oxides that precipitate on the near surface region in high purity single crystals of platinum and the conditions of their preparation are discussed in some detail. We show that these oxides, once formed, are stable indefinitely below 400-500°C because of the very slow rate of decomposition that is controlled by the diffusion of oxygen from the bulk of the noble metal to its surface. Like many other solid state systems, the thermodynamically metastable compounds are stabilized by the very slow kinetics of re-equilibration in the solid phase.

The existence of oxides of other noble metals that are also kinetically stabilized under conditions where they are thermodynamically unstable are also discussed. The influence of defects and impurities on oxide formation is also reviewed.

Experimental

The platinum crystals used in these studies were cut from platinum single crystal rods furnished by Metals Resarch Corporation. Various ultrahigh vacuum systems were employed in the course of these investigations that were equipped with a retarding field analyzer (RFA), or a cylindrical mirror analyzer (CMA), for Auger electron spectroscopy studies (AES) of the surface composition. Control of the gases in the chamber was accomplished in each case by mass spectrometers of the quadrupole type. The temperature of the crystals was measured by means of chromel-alumel thermocouples spot-welded to the edge of the crystals. These studies were carried out using two samples of (111) orientation, one stepped (332) surface and one (110) orientation crystal surface. The structure of the metal crystal surfaces and of the

ordered oxides was studied by low energy electron diffraction (LEED).

3. LEED and AES Studies of Oxide Structures

3.1 Oxide Preparation In all the crystals investigated, the conditions for oxygen uptake were similar. Initially the crystals were cleaned by a combination of oxygen treatments at >600°C and $P_{O_2} \sim 10^{-7}$-10^{-6} Torr and argon sputtering, followed by flashing above 1000°C. The LEED patterns showed in each case the corresponding structures due to the clean crystal surfaces, and the Auger spectra showed no other peaks than those of the platinum substrate. This cleanliness requirement is very important as the presence of impurities such as Si and Ca lead to their preferential oxidation (21), often preventing the formation of oxides of the noble metal.

Oxygen was then admitted into the UHV chamber up to a pressure in the range of 10^{-6}-10^{-5} Torr, while the sample crystal was maintained at temperatures above 700°C. After 30 minutes, the oxygen gas phase was removed and the crystal was allowed to cool to room temperature. Auger peak ratios, $O_{506}/Pt_{237} \sim 1$ were measured by AES at this stage in some of the crystals. This value corresponds to the presence of more than a monolayer of oxygen as determined by the quantitative studies of Biberian et al. (45) This value decreased in the different samples after heating in vacuum to produce the ordered LEED patterns.

We have often observed a considerable variation in the ease with which oxygen can be incorporated into the crystal. In general, clean and well annealed crystals that have been kept in the UHV chamber for long periods of time are more difficult to oxidize. In these cases we have found that an effective way to incorporate oxygen into the lattice consists of Ar bonbarding the crystal at 2 KeV and then annealing it in the presence of oxygen using the conditions

of oxidation described above. Also, when removing C deposits on the Pt surface by reaction with O_2, oxygen incorporation into the metal occurs after the removal of the carbon. Finally, crystals that have been exposed to air for a long time are also found to oxidize more readily.

Results

Pt(111). Two different Pt(111) crystals were studied in two different vacuum systems. The results of oxidation studies for these crystals will be described separately.

The first crystal was studied in a system with a single pass CMA. After exposing the sample to oxygen at 800°C for approximately 10 minutes, the crystal was briefly flashed to 1000°C in vacuum. The Auger spectrum taken after this rapid heat treatment is shown in Figure 1 with a 3 Vpp modulation. As can be seen in the figure, oxygen is the only element present apart from platinum. A small peak at 92.5 eV is present which is probably due to the platinum substrate (silicon also has a peak at this energy). No peaks could be seen at the energies corresponding to oxidized silicon around 76 eV and 83 eV or due to calcium contamination as shown by the absence of any detectable feature at around 293 eV.

After the short flash the crystal showed the complex LEED pattern of Figure 2a and 2b. The pattern could be interpreted as a superposition of several oxide structures, I, II, and III, that formed domains over the (111) platinum substrate. In Figure 2d, we show separately one of these domains for more clarity. In structure I, the two domains rotated ± 14.2° with respect to the substrate show a compression of the unit cell length of approximately 3% with respect to the parallel oriented domain. We distinguish them by subscripts Ia (parallel orientation) and Ib (± 14.2° rotation). The length of the measured unit cells and rotation angles with respect to the (111) substrate

are summarized in Table I.

When measuring the unit cell lengths, use was made of the high order diffracted beams of each structure that were closest to the integral substrate beams in order to minimize distortion effects that arise from imperfections in the retarding grids, residual magnetic fields, and imperfect positioning of the crystal in the center of curvature of the LEED optics. The estimated uncertainty in the measured unit cell lengths is ±0.15 Å . All of the observed structures display hexagonal symmetry. The thickness of the different oxide domains is probably a few atomic layers, as indicated by the absence of double diffraction features at this stage. Real space models for structures I, II, and III are shown in Figure 3.

On repeating the same experiment (flashing to 1000°C then cooling in vacuum) we could obtain again most of the the structures shown in Figure 2, although the relative intensities and rotation angles depended on the annealing temperature and time. Structure IV, for example, showed orientational disorder upon heating to 1025°C for a short time as shown by the streaked ring-like structure of Figure 4.

Other structural changes that occured upon short flash of the crystal to different temperatures led to the formation of structures that are higher multiples of structure II or IV. Loss of oxygen is observed to occur in the successive flashes to high temperatures. Two of the domains of structure II give rise to double diffraction features, as seen in Figure 4. This indicates that at this stage the thickness of these domains has decreased to a few atomic layers.

A third, short flash to 1040°C left only two domains of structure I and produced another structure, which is shown in Figure 5. This new structure has a unit cell which appears to be a multiple of the unit cells of

either structure III or IV as indicated in Table I. A final flash to >1100°C for a few minutes removed all structures as well as the oxygen from the platinum crystal.

The second Pt(111) crystal was studied in a UHV system that was equipped with a retarding field analyzer. The crystal was cleaned and exposed to O_2 for 30 minutes at 700°C.

Upon cooling the crystal and removing the gas phase oxygen, the oxygen to platinum Auger peak ratio was near unity again. No silicon or calcium impurities could be detected by AES.The LEED pattern showed a diffuse 1x1 structure. After flashing the crystal to >800°C for a few minutes, the patterns of Figure 6 were obtained. The ratio of Auger intensities remained unchanged after this treatment. The pattern of Figure 6a was present in the center of the crystal, and that of Figure 6b only near the edge of the crystal. The presence of steps in this edge region is apparent by the doublet structure of the integral order beams. The unit cell length and rotation angles of these three domain structures is summarized in Table I. Essentially, the structures are the same as structure IV, on the previous Pt(111) crystal, although the rotation angles are different and do not show the disorder observed in that case. It is interesting to note that the presence of steps stabilizes a single domain structure rotated 30° with respect to the substrate. This is seen more clearly in the oxides formed on a stepped crystal as described in the next section.

Pt(332) or Pt(S)-[6(111)x(111)]. This crystal face, when clean and ordered, has (111) orientation terraces of about six atoms in width, separated by steps of monatomic height and (111) orientation as revealed by LEED. Annealing the oxidized crystal to >800°C for several minutes produced the LEED patterns of Figure 7a and 7b. The structures were not uniformly present

on the surface, but formed patches. The stepped structure became highly disordered as evidenced by the continuous streaks that connect the initially doublet spots. By contrast, the spots in both oxide structures are sharp, indicating the formation of enlarged (111) terraces due to faceting of the surface. In the regions giving rise to the pattern of Figure 7a (structure IV) one single domain is observed while two domains, with periodicities (4x2) multiples of the previous one, are observed in the pattern of Figure 7b. The presence of steps blocks the formation of the third domain. Structure IV of Figure 7a is identical to that observed in the two Pt(111) crystals.

Pt(110). After an oxygen treatment similar to those described previously, and a heating period in vacuum of 15 hours at <600°C, the surface of the Pt(110) crystal shows patches with the LEED structure of Figure 8. The Auger spectrum taken with the RFA shows only oxygen in very small amounts. The ratio of oxygen to platinum Auger peaks was 1/30 at this stage. This value, however, is not indicative of the oxygen content of the oxide domains since clean platinum regions are also sampled within the area covered by the electron beam. The structure results from double diffraction from two domains with unit cells as shown in Figure 8. This structure is again identical to that formed on the other crystals of (111) and (332) orientation. The presence of only two domains is not surprising in view of the lower rotation symmetry of this platinum crystal surface. Also, as seen in Figure 8, the clean regions of the Pt(110) substrate showed a (1x2) pattern characteristic to the reconstructed metal surface with a considerable degree of disorder along the [001] direction as evidenced by the elongated half-order spots. Table I summarizes the unit cell lengths and rotation angles.

The Kinetics of Diffusion and Desorption of Ar Imbedded in Pt(111)

As will be argued in the discussion section, one important parameter which controls the decomposition of oxide layers is the slow diffusion of oxygen atoms through the platinum matrix. To illustrate this important effect, we have studied the desorption of argon that has been implanted in the subsurface region of a Pt(111) single crystal as a consequence of argon ion bombardment. The Auger analysis was performed with a CMA. After several minutes of argon bombardment at 10^{-5} Torr and 1 KeV or 2 KeV energy, the crystal shows an argon Auger peak with an intensity which depends on the argon pressure employed during bombardment, the ion current, and accelerating potential. In a typical experiment, the initial argon peak is found at 218 eV (minimum in the dN/dE curve).

Two different heating schedules were used to desorb the implanted argon. In the first, the crystal was heated stepwise with a dwell time of approximately 1 minute at each temperature while the Auger spectrum was being recorded. The ratio of peak heights of argon (218 eV) and platinum (237 eV) is plotted as a function of temperature in Figure 9a. The important observation is the increase in the argon peak intensity, which shows a maximum for that particular experiment, between 800° and 900°C, and then decreases until complete removal of the argon at temperatures above 1000°C. The temperature at which the maximum Auger peak intensity due to argon appears, depends on the dwell time and was not investigated in detail.

In the second heating schedule the temperature of the crystal was rapidly increased to 930°C and then maintained constant. The decrease of the argon Auger peak intensity as a function of time is shown in Figure 9b for two different sputtering energies of 1 KeV and 2 KeV. For the 1 KeV experiment there is a rapid decrease in argon signal that occurs in the

first 60 seconds, followed by a much slower decrease that leads to complete removal of argon for times longer than 30 minutes. For the higher sputtering energy, 2 KeV, the results shown in Figure 9b indicate that heating periods of the order of one hour are necessary to remove the implanted argon.

Discussion

Thermodynamic stability of noble metal oxides. At high temperatures, the dissociation oxygen pressure of even the most stable platinum group oxides would be large enough to eliminate the oxide phases. This is illustrated in Figure 10, where the calculated temperature of oxide equilibrium with 10^{-6} Torr of oxygen is plotted as a function of atomic number for the different transition metals. Thermodynamic data for the calculation of the equilibrium pressure and temperature were obtained from the Handbook of Physics and Chemistry (22) and from other sources (3,23-26). While the 3d transition metal oxides are stable in this circumstance, all 4d and 5d transition metal oxides are unstable in vacuum above 600°C. This result does not depend dramatically on the chosen pressure of 10^{-6} Torr. At 10^{-1} Torr, for example, the temperatures at which the oxides would decompose are increased at most by 200 K. In spite of this thermodynamic instability, penetration of oxygen into the bulk (4,27-32,46) and the formation of oxides in the near surface region of the noble metals has been reported in many surface studies. These include the surfaces of Ir(110) (17), Ir(111) (16), Pt(111) (8,10-13,33), Pt(100) (13), Pt(110) (9,12), Rh(111) (18), Pd(111) (19), polycrystalline Pd (32), Ru(101) (31), and Au(111) (20). Under the conditions of oxide preparation described, there is significant solubility of oxygen in the metal phases which would increase with increasing temperature. At high enough temperatures, to ensure rapid diffusion of oxygen through the

metal, the concentration of oxygen would vary with changing oxygen pressure or changing temperature to maintain the equilibrium oxygen concentration in the metal. Upon rapid cooling of a solid solution of oxygen in the metal, the diffusion rate of oxygen would be reduced to a level where equilibrium between the metal and the gas phase would not longer be maintained. Unfortunately, diffusion data for oxygen are scarce in the litterature for the noble metals. For oxygen, diffusion in platinum, the following values have been reported (34) for the diffusion constant, D_o, and the activation energy, E. D_o = 9.3 ± 1.8 cm^2/s, E=78.0 ± 25.0 kcal/mole. From these values an average time, t, for displacement of oxygen by diffusion along a given distance can be calculated using the formula for random work displacement, $x = 2\sqrt{Dt}$. For 20 Å the following values for t are obtained: $2x10^{-4}$sec at 1200°C, 0.14 sec at 900°C, 2 hrs at 600°C, and 10^5 yrs at 300°C. These figures are by no means accurate in view of the large uncertainties in the value of the reported activation energy and because of the limited temperature range in which the diffusion experiments were carried out (1435°C-1504°C). They do illustrate, however, the slow rate of removal of the oxygen accumulated in the bulk near the surface. The slow desorption of argon implanted in platinum illustrates this point as can be seen in Figure 9b. At 2 KeV sputtering energy, the desorption time is about 1 hour, even at temperatures as high as 930°C.

As the equilibrium solubility decreases rapidly with decreasing temperature, the cooled noble metal sample would be supersaturated and would have an oxygen concentration corresponding to equilibrium with an enormous oxygen pressure. The cooled solid solution would be metastable with respect to ordered oxide phases. Although diffusion would be too slow to allow the

oxygen to move to the surface and vaporize, very small shifts in position could yield various ordered arrangements of the oxygen atoms. There would be a number of ordered oxide phases that would be stable relative to the disordered solution of oxygen in the metal. Some of the possible oxide phases might be thermodynamically unstable with respect to disproportionation to other oxide phases. However, because of the restriction on extensive motion of the oxygen atoms, metastable oxide phases, which would require less motion of the oxygen atoms, can predominate over the stable oxide phases. Once the oxide has been formed, it may be virtually impossible to remove it even at temperatures as high as 600°C or higher. This kinetically controlled oxide stability is certainly more likely to be an important phenomenon in single crystals due to the lack of easy pathways for oxygen diffusion than for polycrystalline samples that are full of grain boundaries.

In summary, the much higher solubility of gaseous oxygen in platinum group metals at high temperatures can result in quenched samples that are highly supersaturated in oxygen. The surface oxygen may be able to escape at the low temperature, but migration from lower layers would be too slow. The supersaturated solution has a much higher Gibbs energy than do the oxide phases at lower temperatures, and there is a strong driving force to produce ordered oxides.

The Structure of Subsurface Platinum Oxides. An interesting characteristic of all the LEED structures found upon the formation of the oxides is the hexagonal symmetry displayed by their diffraction patterns. A variety of oxide structures can be obtained. Upon further heating the crystals, two different phenomena contribute to the elimination of the less stable oxide structures. One is the progressive oxygen depletion from the

crystal lattice, and the other is the formation of more stable ordered oxides. There are changes in the relative orientation of the oxides with respect to the substrate as well as reconstructions within ordered domains. This is the case of structures Ia, Ib, III, IV, and possibly V, as shown in Figures 2-5 and also in Table I. A long heating period is required for the most stable of the oxide structures to grow while the less stable ones disappear. If the supply of oxygen from the deep subsurface layers is exhausted as a result of desorption, the formation of one-domain oxide structures may not be obtained. This seems to be the case with the first Pt(111) crystal after the short exposure to oxygen utilized in that particular case. In other cases, however, when the oxygen supply is abundant, a single oxide structure has been formed, as shown in Figures 6, 7, and 8.

In order to interpret the different structures observed, with the unit cell lengths shown in Table I, we have considered the hexagonal planes of the known platinum oxides. In recent papers on the formation of these oxides (2), it is reported that two oxides are formed with stoichiometries of PtO_2 and Pt_3O_4. Other oxide stoichiometries have also been produced by sputtering film deposition; these include PtO, $PtO_x(1<x<2)$ and Pt_5O_6 (35-37). PtO_2 is shown to grow in two different structures. The α PtO_2 crystal phase is hexagonal with the (0001) basal planes composed of platinum atoms with a separation of 3.10 Å . The other phase of PtO_2 is the β -phase with an orthorhombic unit cell of dimensions 4.486, 4.537, and 3.138 Å . PtO and Pt_5O_6 have tetragonal (a=3.04 Å , c=5.34 Å) and monoclinic (a=5.24 Å , b=5.51 Å , c=11.04 Å , β =94°53') unit cells (35). These phases do not fulfill the requirements of symmetry observed in our LEED patterns and are thus disregarded.

The other candidate to explain the structure of the platinum

oxide that forms in the near surface region of our single crystals is Pt_3O_4 which crystallizes in the cubic system with unit cell dimensions (2) of 5.585 Å . The two-dimensional unit cell on the (111) plane has a dimension of 8.81 Å . Schematic diagrams of both the (0001) plane of α-PtO_2 and the (111) plane of Pt_3O_4 are shown in Figure 3 superimposed on the Pt(111) sustrate.

These two planes have another characteristic that makes them good candidates for our surface oxides. This is the layered Pt-O-O-Pt structure which is in accordance with ion scattering observations (38), indicating that the oxygen atoms are below the first platinum layer. The possibility of these oxides to become non-stoichiometric by loss of oxygen could explain the ease with which reconstructed domains appear in the diffraction patterns. The good agreement between the measured unit cell dimensions shown in Table I and the dimensions of the hexagonal plane unit cells of α-PtO_2 and Pt_3O_4 supports the assignment proposed in the Table.

It should be mentioned at this point that in an earlier study of the oxidation of Pt(111) crystals (10) at much higher oxygen pressures (500 Torr) than those used in this work, the observed LEED patterns were very similar to the ones reported here. These higher oxygen pressures produced structures also summarized in Table I.

The oxide LEED pattern from Pt(110) shown in Figure 7 has also been reported previously (12). The interpretation given by the authors for this structure, however, is a (3x12) coincidence pattern which does not correlate with our measurements of the unit cell dimensions in Figure 8.

Can Impurities Influence the Formation of Noble Metal Oxides?

Impurities in the noble metal crystal lattice, when present in large amounts, may act as a getter for oxygen that is dissolved in the metal matrix.

In this circumstance it might be more difficult to precipitate the noble metal oxides while the impurity oxide phase would readily form. An example of this effect is the segregation of silicon oxides in platinum single crystals that occurs when the silicon contaminated noble metal is exposed to oxygen (14, 15, 21). Other examples include the possible formation of compounds like $CaPt_2O_4$ or CaO that segregate also to the surface of platinum upon exposure to oxygen (47). However, the surface segregation and oxidation of impurities at noble metal surfaces cannot explain the oxide structures formed in the near surface region of platinum reported in this paper and by others in the absence of detectable impurities. In this study special care was taken to ascertain the cleanliness of the platinum surfaces throughout our investigations. As mentioned before, no impurities, including calcium or silicon, were detectable by Auger spectroscopy in the platinum crystals that were used. In order to check if undetected amounts of either silicon or calcium might be responsible for the observed structures, we also compared our measured unit cell dimensions with the ones expected from platinum compounds with oxygen and silicon or calcium.

In a recent work using X-ray diffraction diffraction techniques, the reaction of PtO_2 with other metal oxides was examined (40). It was found that in the case of the SiO_2-PtO_2 system there was no evidence for compound formation or solid solution, even at temperatures as high as 1200°C. Rather, SiO_2 precipitates in a separate phase as coesite. Also, all unit cell dimentions are incompatible with those of SiO_2 crystal planes of hexagonal symmetry. In the case of calcium componds, the proposed $CaPt_2O_4$ is tetragonal with unit cell dimensions (41), a=5.778 Å and c=5.599 Å . Clearly, no low index plane of hexagonal symmetry exists in this structure. Another calcium compound that was not considered in that work, but was

reported elsewhere (41), is $CaO \cdot PtO_2$ with a hexagonal unit cell of dimensions a=9.328 Å and c=11.244 Å . It is clear that none of these compounds can explain the observed unit cell lengths and are ruled out also by the lack of silicon or calcium Auger signals in our spectra. It is important to note that the ratio of calcium and oxygen Auger peaks observed in CaO (42) is [Ca(239 eV)/O(510 eV)] = 1.31, making the observation of calcium by AES even easier than that of oxygen.

A recent study (44) of rhodium oxides shows how small changes in chemical composition can stabilize the metastable noble metal oxide. When Rh_2O_3 is used as a catalyst in a reducing mixture of CO and H_2 gases at 6 atm, it reduced readily (within an hour) to the metallic state at 300°C. However, when the hydrated oxide, $Rh_2O_3 \cdot 5H_2O$ was employed as a catalyst under the same reaction conditions, the rate of reduction was greatly diminished and the oxide catalyst remained stable for days.

An important catalytic effect that may also be exhibited by small amounts of impurities would stabilize the oxide structures as reported by recent studies of the adsorption of oxygen by Au(111) single crystals (39,43). The effect of calcium in promoting dissociation and adsorption of oxygen was pointed out. "Spillover" of the dissociated oxygen atoms from the calcium oxide phase into gold was invoked to explain the increase in oxygen signal by AES (43).

A quite different effect is the stabilization of the metastable noble metal oxide structures that may occur as a result of compound formation under appropriate experimental conditions.

Acknowledgement: This work was supported by the Director, Office of Energy Research, Office of Basic Energy Sciences, Materials Sciences Division of the U.S. Department of Energy, under Contract W-7405-ENG-48; and by the Spanish-American Cooperative Program.

References

1. J.C. Chaston, Plt. Metals Rev. 8, 50 (1964).
2. O. Muller and R. Roy, J. Less Common Metals 16, 129 (1968).
3. R.J. Berry, Surf. Sci. 76, 415 (1978).
4. J.P. Hoare, Electrochimica Acta 26, 225 (1981)
5. R. Thacker and J.P. Hoare, J. Electroanal. Chem. 30, 1 (1971).
6. J.P. Hoare, R. Thacker, and C.R. Wiese, J. Electroanal. Chem. 30, 15 (1971).
7. S.M. Davis and G.A. Somorjai, Surf. Sci. 91, 73 (1980).
8. R.W. McCabe and L.D. Schmidt, Surf. Sci. 65, 189 (1977).
9. R.W. McCabe and L.D. Schmidt, Surf. Sci. 60, 85 (1976).
10. B. Carriere, P. Legare and G. Maire, J. Chimie Physique 71, 355 (1974).
11. B. Lang, R.W. Joyner, and G.A. Somorjai, Surf. Sci. 30, 454 (1972).
12. R. Ducros and R.P. Merrill, Surf. Sci. 55, 227 (1976).
13. G. Maire, P. Legare, and G. Lindauer, Surf. Sci. 80, 238 (1979).
14. H. Niehus and G. Comsa, Surf. Sci. 102, L 14 (1981);
15. H.P. Bonzel, A.M. Franken, and G. Pirug, Surf. Sci. (to be published).
16. H. Conrad, J. Küppers, F. Nitschke, and A. Plagge, Surf. Sci. 69, 668 (1977).
17. J.L. Taylor, D.E. Ibbotson, and W.H. Weinberg, Surf. Sci. 79, 349 (1979).
18. D.G. Castner and G.A. Somorjai, Appl. Surf. Sci. 6, 29 (1980).
19. H. Conrad, G. Ertl. J. Küppers and E.E. Latta, Surf. Sci. 65, 245 (1977).
20. M.A. Chesters and G.A. Somorjai Surf. Sci. 52, 21 (1975).
21. M. Salmerón and G.A. Somorjai (to be published in J.Vac.Sci. & Technol.)
22. Handbook of Physics and Chemistry, 61st ed., CRC Press, ed. R.C. West, The Chemical Rubber Co. Cleveland, 1980.
23. H.H. Kellogg, J. Chem. Eng. Data 19, 41 (1969).
24. G. Bayer and H.G. Wiedemann, Thermal Analysis 1, 763 (1974) Proc. Fourth ICTA, Budapest, 1974.
25. D. Chatterji and R.W. West, J. Am. Ceramic Soc. 54, 73 (1970).
26. H.J. deBruin and S.P.S. Badwal, J. Solid St. Chem. 34, 133 (1980).
27. P.A. Thiel, J. T.Yates Jr., and W.H. Weinberg, Surf. Sci. 82, 22 (1979).

28. D. L. Weissman, M. L. Shek, and W.E. Spicer, Surf. Sci. 92, L59 (1980);

29. P.A. Zhdan, G.K. Boreskov, A. T. Boronin, W.F. Egelhoff, and W.H. Weinberg, Surf. Sci. 61, 25 (1976)

30. V.P. Ivanov, G.K. Boreskov, V.I. Savchenko, W.F. Egelhoff, and W.H. Weinberg, Surf. Sci. 61, 207 (1976).

31. P.D. Reed, C.M. Comrie and R.M. Lambert, Surf. Sci. 64, 603 (1977).

32. C.T. Campbell, D.C. Foyt and J.M. White, J. Phys. Chem. 81, 491 (1977).

33. J.L. Gland, B.A. Sexton, and G.B. Fisher, Surf. Sci. 95, 587 (1980).

34. L.R. Velho, and R.W. Bartlett, Met. Trans. 3, 65 (1972) [cited in Diff. Data 6, 56 (1972)].

35. M. Hecq, A. Hecq, and J.P. Debrue, J. Less Common Metals 64, P25 (1979).

36. M. Hecq and A. Hecq, J. of Less Common Metals 56, 133 (1977).

37. M.C. Canart-Martin, J.P. Delrue, L.D. Laude, and M. Wautelet, Chem. Physics 48, 283 (1980).

38. H. Niehus and G. Comsa, Surf. Sci. 93, L 147 (1980).

39. P. Legare, L. Hilaire, M. Sotto and G. Maire, Surf. Sci. 91, 175 (1980).

40. H.R. Hoekstra, S. Siegel, and F.X. Gallagher, Adv. Chem. Ser. 98, 39 (1971).

41. C.L. McDaniel, J. Am. Cer. Soc. 55, 426 (1972).

42. A. Shih, C. Hor, and G.A. Haas, Appl. Surf. Sci. 2, 112 (1979).

43. M.E. Schrader, Surf. Sci. 78, L 227 (1978).

44. P.R. Watson and G.A. Somorjai, submitted to J. Catal.

45. C.E. Smith, J.P. Biberián, and G.A. Somorjai, Surf. Sci. 57, 426 (1979).

46. M. Salmerón and G.A. Somorjai, Surf. Sci. 91, 373 (1980).

47. G. Lindauer, P. Legare, and G. Maire, Proc. ECOSS 3, Vol.1, 537 (1980).

Figure Captions

Figure 1. Auger sectrum from the Pt(111) crystal face after 10 minutes exposure to 10^{-6} Torr of O_2 at 800°C, followed by a short flash to 1000°C. The spectrum was taken with a modulation amplitude of 3 Vpp.

Figure 2. LEED patterns of Pt(111) treated in O_2 and flahsed to 1000°C. (a) E=30 eV, (b) E=45 eV, (c) Schematic diagram corresponding to (a) showing the various domains: Structure I has three rotated domains (O, ⊙, Θ); structure II also has three domains (▲ ▲ Δ); structure III has two domains (□ , ⊡). One of the domains of structure I (⊙), is shown in diagram (d) separately for clarity.

Figure 3. Real space unit cell models for structues I, II, and III. In each diagram, open circles represent substrate Pt(111) atomic positions. Filled circles represent atomic positions of Pt atoms in the (0001)-PtO_2 plane in (a), (b), and (e), and in the (111)-Pt_3O_4 plane in (c) and (d). Large filled circles mark the positions of atoms in the real space unit cell that correspond to the LEED pattern of Fig. 2. (a) Structure Ia; (b) Structure Ib; (c) Structure II (metal substrate and oxide domain parallel); (d) Structure II, (oxide domain rotated 24.5°); (e) Structure III.

Figure 4. (a) LEED pattern from a Pt(111) crystal treated in O_2 and flashed to 1000°C for a few seconds. Structure IV develops as disordered domains as shown by the dashed lines in (b). Other modifications that occur are the appearance of double diffraction features around the substrate first order spots (b). (c) and (d) are real space models for two domains of Structure IV.

Figure 5. (a) LEED pattern from Pt(111) treated in O_2 after a flash to 1040°C, E=46 eV. (b) Schematic diagram of (a) shows the appearance of a new structure, V , with two domains (open and filled circles). Large circles correspond to intense spots and small circles to weak spots. (c) One domain of structure V is shown separately for clarity.

Figure. 6 LEED patterns of Pt(111) after O_2 treatment and flash to >800°C for a few minutes. (a) Diffraction from center of the crystal at E=65 eV; (b) Diffraction from the edge region at E=74 eV showing a third domain due to the presence of steps; (c) and (d) are schematic diagrams for (a) and (b); (e) two domains of the IV structure are shown in real space. Open circles represent atomic positions of the underlying Pt(111) substrate.

Figure 7. LEED patterns from Pt(332) treated in O_2 and annealed at >800°C for several minutes. The patterns (a) at E=62 eV, and (b) at E=105 eV corresponding to structure IV are present in some regions of the surface, while pattern (c) at E=110 eV is present in other regions (structure VI); (d) and (e) are schematic diagrams corresponding to (b) and (c). Real space unit cell dimensions of structures (IV and VI). Only one domain of structure VI is shown for clarity. Open circles represent substrate Pt(111) atomic positions. The dashed line indicates the direction of the step edges.

Figure 8. LEED patterns from Pt(110) treated in O_2 and annealed at <600°C for 15 hours at electron energies of (a) E=62 eV, and (b) E=122 eV. (c) Schematic diagram of (a) showing the two domains of structure IV. The pattern is formed by double diffraction between the oxide layer and the Pt(110) substrate. For clarity, only the reciprocal lattice points around the (00) spot are drawn. Elongated spots are from the 1/2 order beams of the 1x2 reconstructed domains of the clean platinum patches of the surface. (d) Real space cell dimensions for the two domains (o,x). Open circles represent atomic positions in the Pt(110) plane.

Figure 9. (a) Argon (218 eV) to platinum (237 eV) Auger peak-to-peak ratios as a function of temperature after argon ion implantation in Pt(111) at 2 KeV. (b) Same ratio as a function of time after rapidly increasing the crystal temperature to 930°C, for two ion implantation energies.

Figure 10. Calculated temperature of oxide decomposition that corresponds to an oxygen equilibrium pressure of 10^{-6} Torr for group VIII and Group 1B transition metals. For Os, the oxide OsO_4 is in gaseous form, while for Re the oxide ReO_3 is a liquid at the corresponding temperatures.

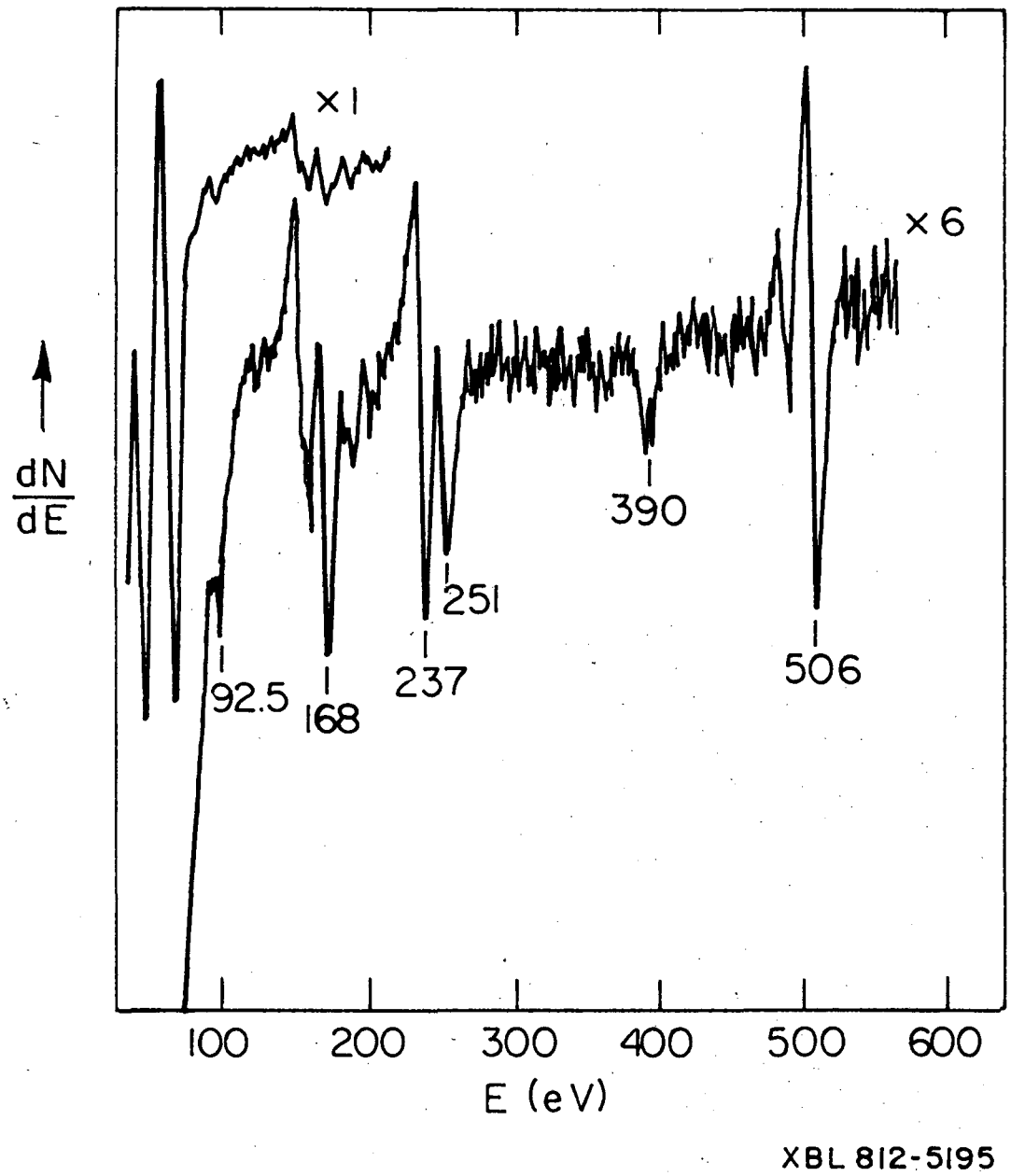
×1
×6
dN/dE
92.5
168
237
251
390
506
100
200
300
400
500
600
E (eV)
XBL 812-5195

Fig.1

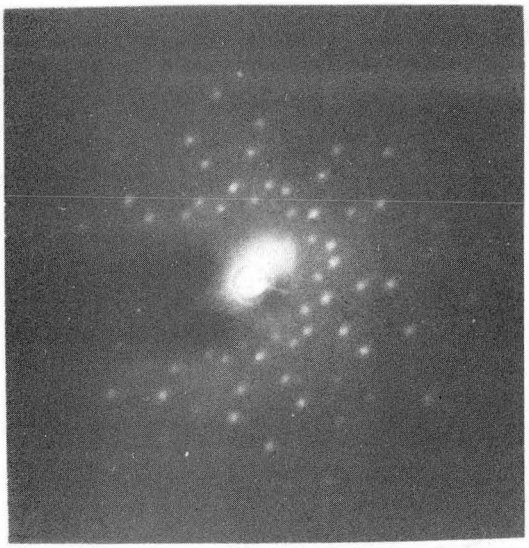

a

b

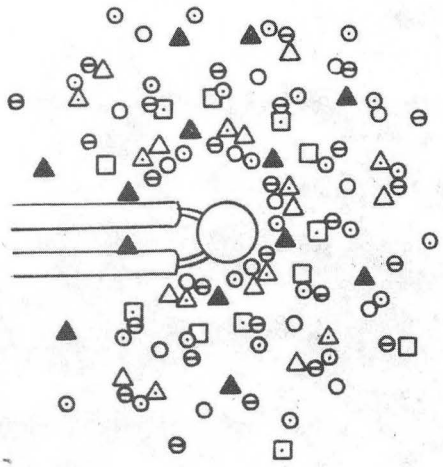

c

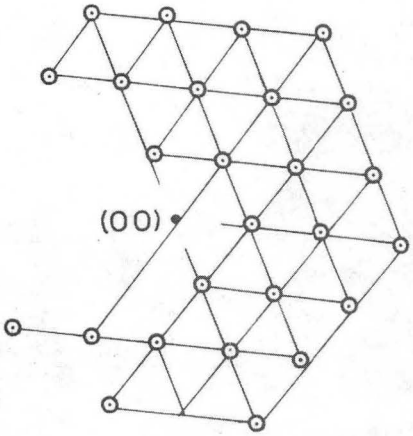

d

XBB 813-2817

Fig.2

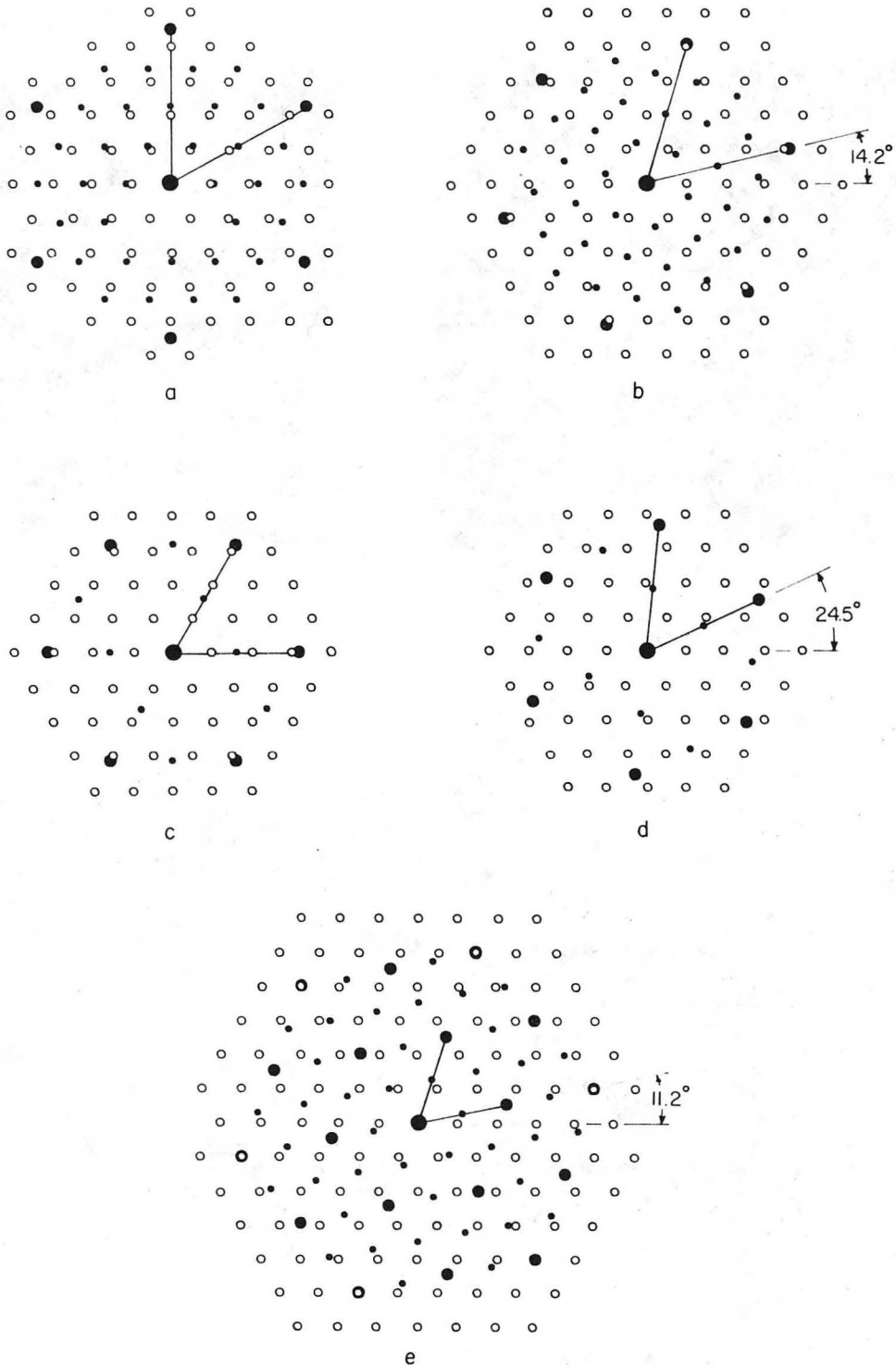

XBL813-5339

Fig.3

a

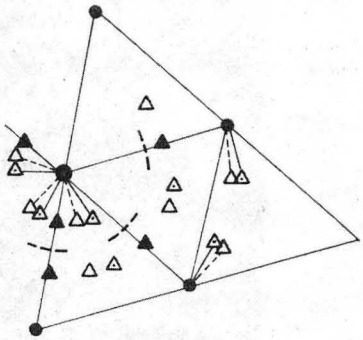

b

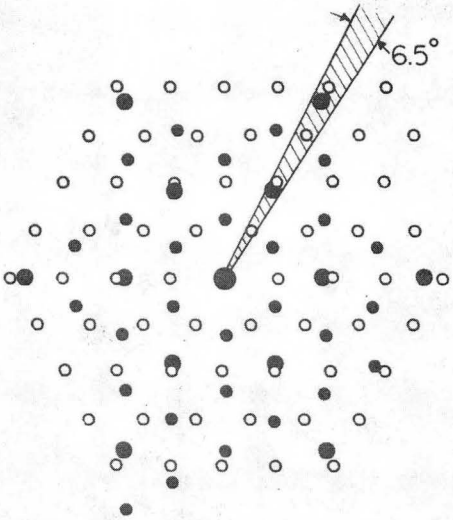

c

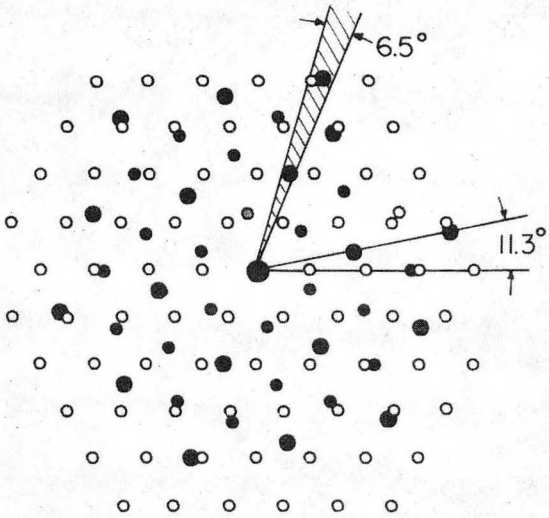

d

XBB 813-2818

Fig.4

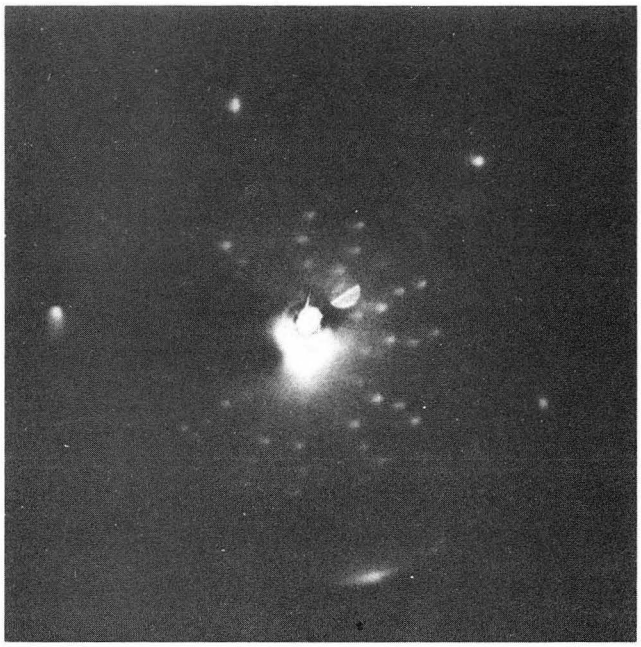

a

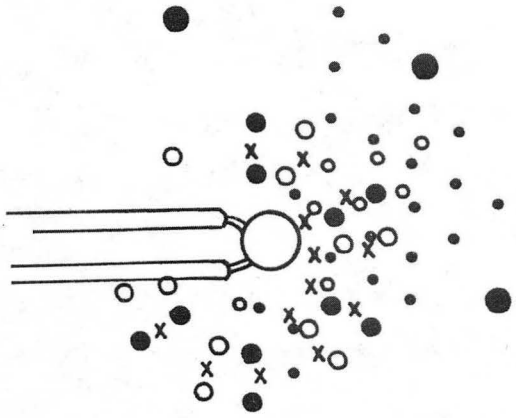

b

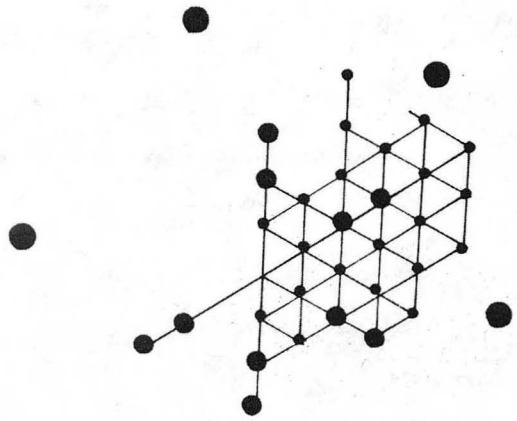

c

XBB 813-2816

Fig.5

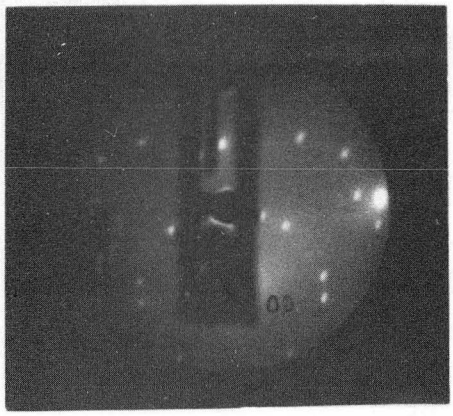

a

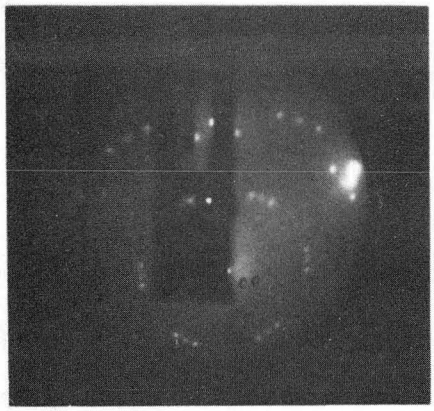

b

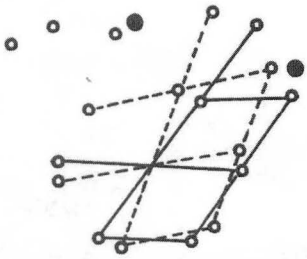

c

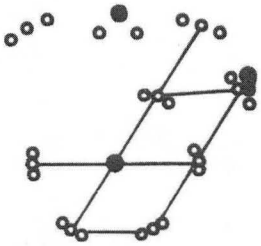

d

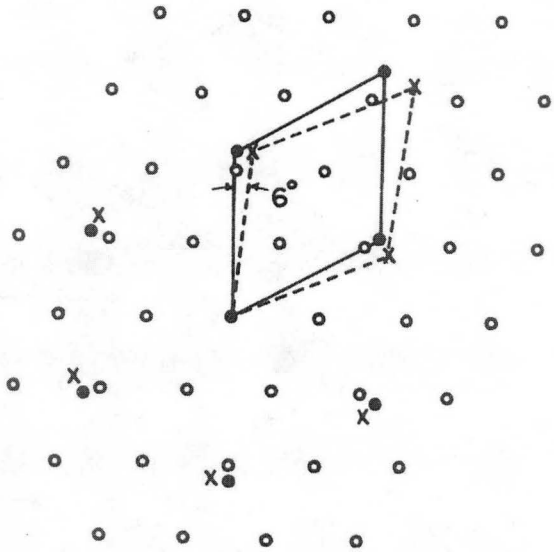

e

XBB 800-14485

Fig.6

a b c

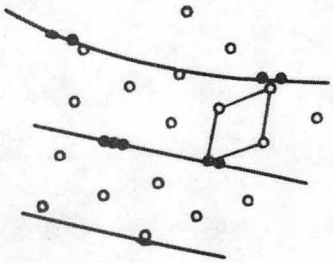

d

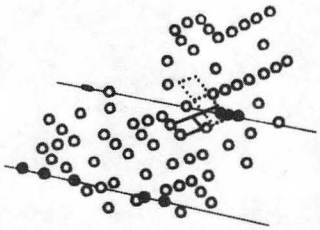

e

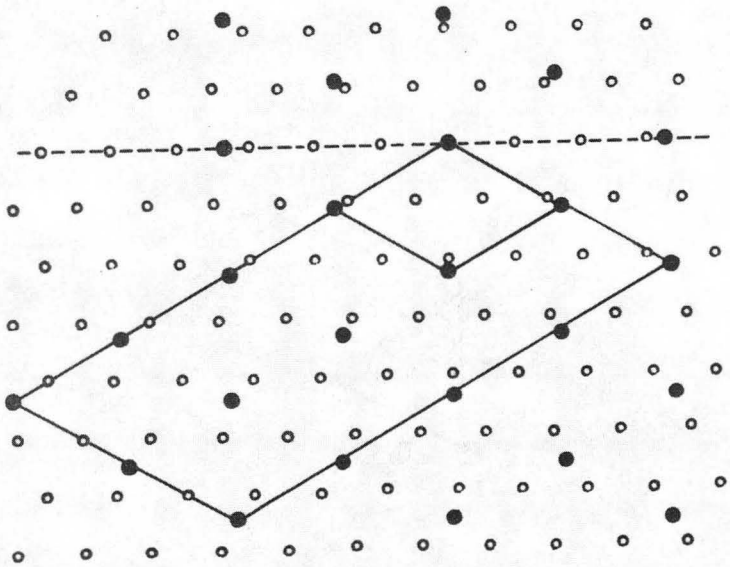

f

XBB-800-14484

Fig.7

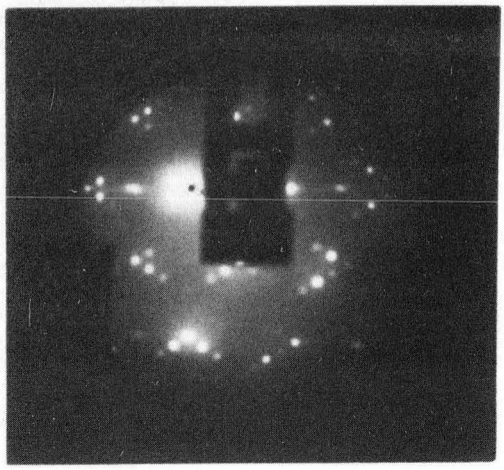

a

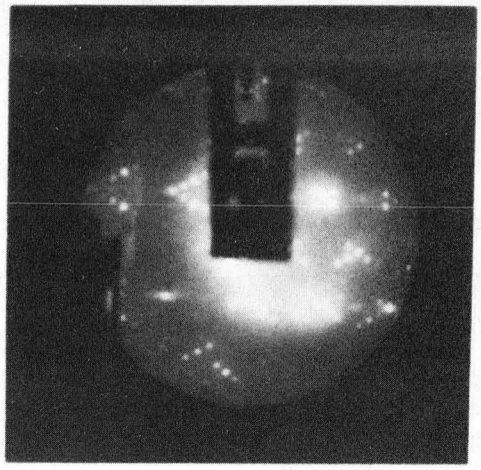

b

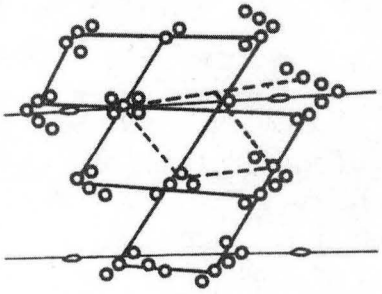

c

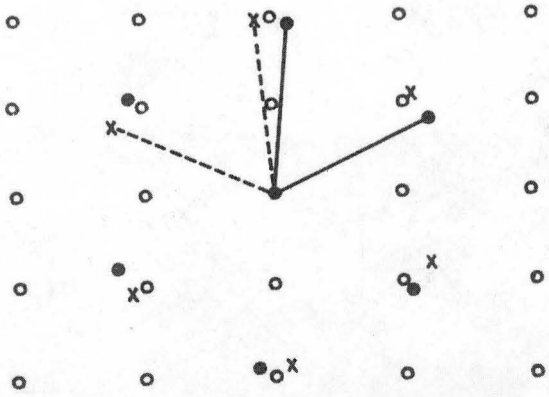

d

XBB 800-14486

Fig.8

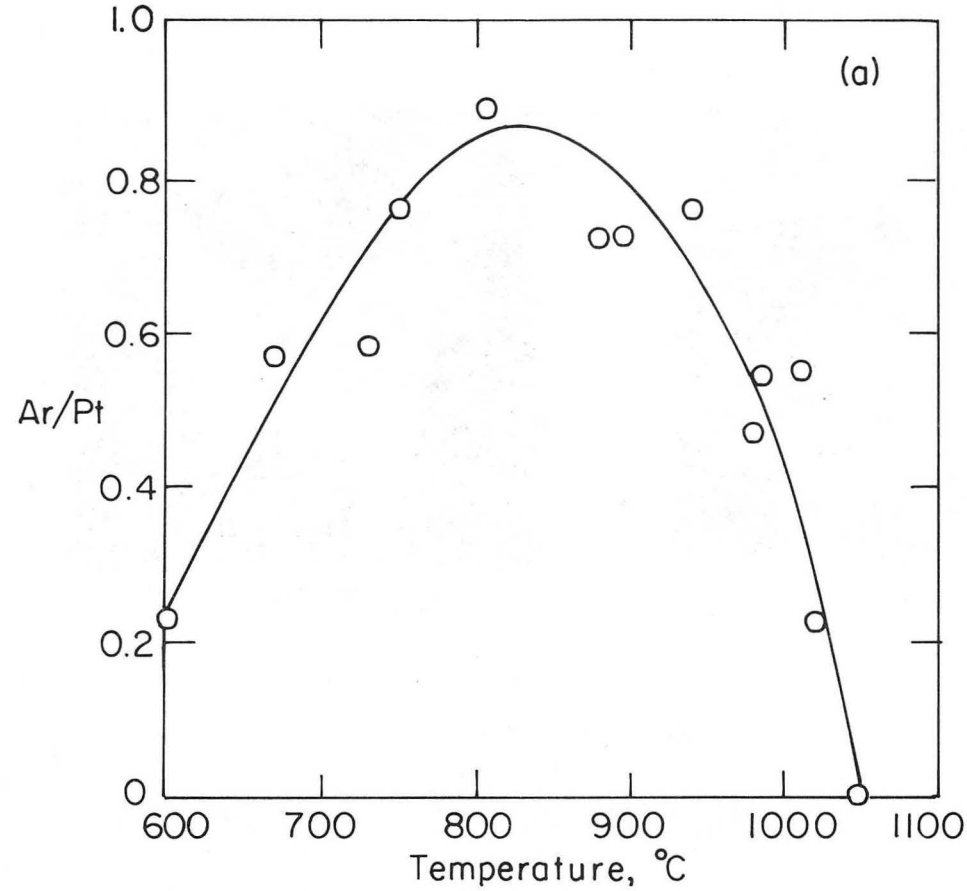

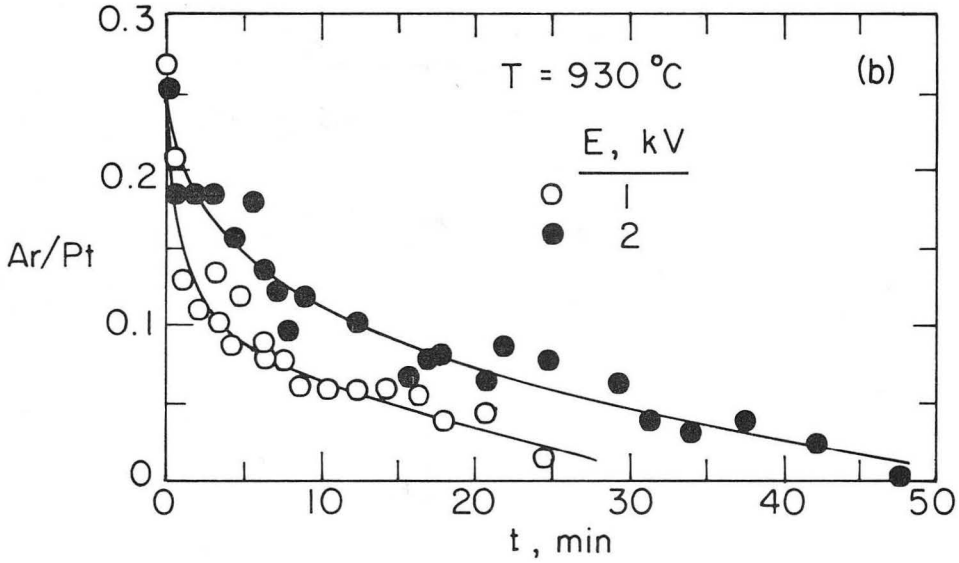

XBL 813-5338

Fig.9

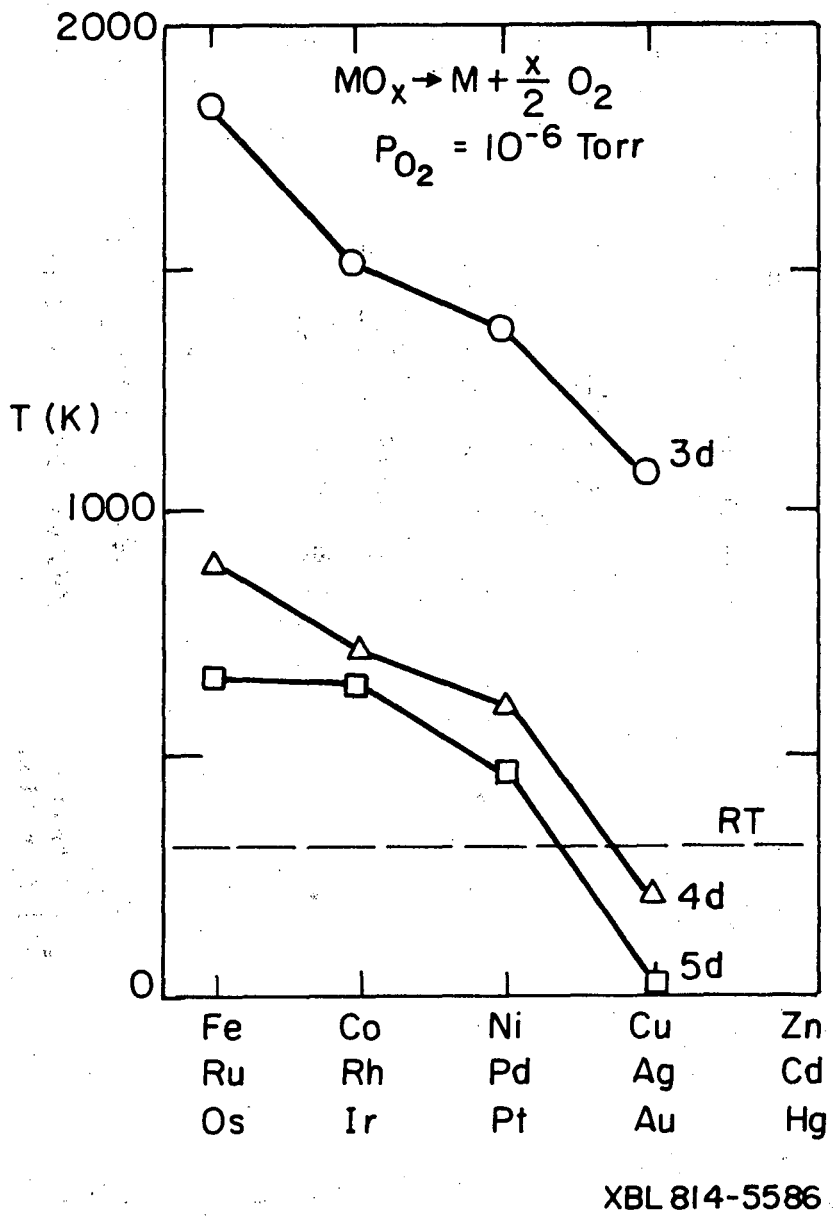
2000
1000
0
T (K)
$MO_x \rightarrow M + \frac{x}{2} O_2$
$P_{O_2} = 10^{-6}$ Torr
3d
4d
5d
RT
Fe Ru Os
Co Rh Ir
Ni Pd Pt
Cu Ag Au
Zn Cd Hg
XBL 814-5586

Fig. 10

TABLE I

LEED Structures of Platium Surface Oxides

Crystal (this work)	Structure and Measured Unit Cell Length (Å) (± 0.15 Å)		Rotation angle α with respect to substrate	Proposed Oxide Structure	Expected Unit Cell Lengths in Å
Pt(111) No.1	Ia	10.68	0°	$(2\sqrt{3}x2\sqrt{3})R30°-PtO_2(0001)$	10.74
	Ib	10.36	± 24.5°	" "	10.74
	II	8.77	0°, ± 24.5°	$(1x1)-Pt_3O_4(111)$	8.81
	III	6.26	± 11.5°	$(2x2)-PtO_2(0001)$	6.20
	IV	5.27	0°, ± 11.5°(Δα =6.5°)	$(\sqrt{3}x\sqrt{3})R30°-PtO_2(0001)$	5.37
	V	15.30	± 20°	$(5x5)PtO_2(0001)$ or $(\sqrt{3}x\sqrt{3})R30°-Pt_3O_4(111)$	15.50 15.26
Pt(111) No.2	IV	5.31	± 23.2°	$(\sqrt{3}x\sqrt{3})R30°-PtO_2(0001)$	5.37
	IV	5.31	30°	" "	5.37
Pt(332)	IV	5.24	30°	" "	5.37
	VI	21.0, 10.5	30°	$(4\sqrt{3}x2\sqrt{3})R30°PtO_2(0001)$	21.48,10.74
Pt(110)	IV	5.23	± 5.5° from [1$\bar{1}$0] direction	$(\sqrt{3}x\sqrt{3})R30°\ PtO_2(0001)$	5.37

Other Autors'

Pt(111) ref.10 & ref.13	A	5.28	30°	$(\sqrt{3}x\sqrt{3})R30°-PtO_2(0001)$
	B	21.12	30°	$(4\sqrt{3}x4\sqrt{3})R30°-PtO_2(0001)$
	C	--	0°	$(2x2)-PtO_2(0001)$
	D	--	0°	$(1x1)-PtO_2(0001)$
	X	rectangular 19.2, 9.5	3.5°	--
Pt(S) [13(111)x (310)] ref.13	A			$(\sqrt{3}x\sqrt{3})R30°-PtO_2(0001)$
	D			$(1x1)-PtO_2(0001)$
Pt(100) ref.13	A			$(\sqrt{3}x\sqrt{3})R30°-PtO_2(0001)$
Pt(110) ref.12	IV			(110)PtO in (3x12) coincidence with Pt(110) substrate
Pt(S)[6(111) x(100)] Ref.11				Disordered $(0001)-PtO_2$ domains

This report was done with support from the Department of Energy. Any conclusions or opinions expressed in this report represent solely those of the author(s) and not necessarily those of The Regents of the University of California, the Lawrence Berkeley Laboratory or the Department of Energy.

Reference to a company or product name does not imply approval or recommendation of the product by the University of California or the U.S. Department of Energy to the exclusion of others that may be suitable.

TECHNICAL INFORMATION DEPARTMENT
LAWRENCE BERKELEY LABORATORY
UNIVERSITY OF CALIFORNIA
BERKELEY, CALIFORNIA 94720